

Electrolytic Conductivity and Glass Transition Temperatures as Functions of Salt Content, Solvent Composition, or Temperature for LiBF₄ in Propylene Carbonate + Diethyl Carbonate

Michael S. Ding*

Army Research Laboratory, 2800 Powder Mill Road, Adelphi, Maryland 20783

The electrolyte system of LiBF₄ in propylene carbonate (PC) + diethyl carbonate (DEC) was measured for its electrolytic conductivity κ at salt molalities m , solvent mass fractions w , and temperatures θ in the ranges of (0.2 to 2.1) mol kg⁻¹ for m , (0 to 0.7) for w of DEC and (–80 to 60) °C for θ , and for its glass transition temperatures T_g in the same ranges of m and w . The measured $\kappa(m, w)$ data at different θ were further fitted with an extended version of the Casteel–Amis equation in order to correlate the changes of κ with simultaneous changes of m and w and with θ . The κ surfaces according to these fitted equations all assumed a “dome” shape as a result of κ peaking in both m and w . Furthermore, as θ was decreased, these domes reduced in height and shifted in the direction of low m and high w , the direction of lower viscosity η . The T_g was found to increase with increasing m and decreasing w , indicating a concurrent change in the η of the solution. These results are in complete qualitative agreement with those of LiPF₆ in PC + DEC. Quantitatively, however, the T_g of the LiBF₄ solution is lower than that of the LiPF₆ solution, indicating a lower η of the former, and the κ is generally lower because of the stronger ion association of Li⁺ with BF₄⁻ than with PF₆⁻, except at high m and low θ , where the LiBF₄ solution becomes more conductive because of its lower η .

Introduction

This report in large part parallels an earlier one,¹ in both structure and content, that one dealing with electrolytic conductivity (κ) and glass transition temperature (T_g) of the solution of LiPF₆ in propylene carbonate (PC) + diethyl carbonate (DEC) and this one dealing with LiBF₄ in PC + DEC. In addition, this report briefly compares these two solutions for their T_g and κ values, for which a more complete and detailed presentation can be found elsewhere.²

These solutions are two prominent examples of the carbonate-based electrolytes that are widely used in lithium-ion batteries because of their high electrochemical stability, good electrolytic conductivity, and other favorable properties and because of the ease with which these properties can be tailored to particular needs through adjustments of their compositions.^{1,3,4} In addition to PC and DEC, carbonates for this use include ethylene carbonate (EC), dimethyl carbonate (DMC), and ethyl methyl carbonate (EMC), which, along with their mixtures, have been systematically studied for their dielectric constant (ϵ),^{5–13} viscosity (η),^{6–12,14–17} and phase equilibrium,^{4,18–23} with regard to their application to lithium-ion batteries. In the same regard, electrolytic conductivities (κ) of many of the solutions have been measured as functions of salt content (denoted here as molality m), solvent composition (mass fraction w), and temperature (θ /°C or T /K).^{8–12,24–35} But so far, these κ measurements have largely been restricted to those where the dependency of κ on m is studied separately from that on w , with only a few exceptions. Some recent exceptions are the studies on electrolyte systems LiPF₆(m) + (1 – w)EC + w EMC,²⁵

LiPF₆(m) + (1 – w)EC_{0.3}PC_{0.3}EMC_{0.4} + w TFP,⁸ where TFP stands for tris(2,2,2-trifluoroethyl) phosphate, and more recently PC + DEC and PC + EC solutions of LiPF₆,^{1,2,26} in which κ was measured as a function of both m and w at different θ . In the first two cases, the measured $\kappa(m, w, \theta)$ data were fitted successfully with trivariate polynomial functions $\kappa = f(m, w, \theta)$, and in the third, the measured $\kappa(m, w)$ data were fitted with an extended version of the Casteel–Amis equation^{1,26,36} at different θ . These functions when plotted as κ surfaces in m w coordinates greatly helped in the elucidation of the pattern and the mechanisms of the change of κ with simultaneous changes of m and w at different θ .

The aim of this report is first to present a relatively complete set of $\kappa(m, w, \theta)$ data in numerical form for the electrolyte LiBF₄(m) + (1 – w)PC + w DEC in the ranges of m , w , and θ of (0.2 to 2.1) mol kg⁻¹, (0 to 0.7) mass fraction, and (–80 to 60) °C, respectively. This is to complement another paper on the same set of measurements in which space has only been given to the interpretation and application of the results but not to the tabulation of the numerical values.³⁷ Second, it is to provide another set of numerical data of T_g for the electrolyte, insofar as could be experimentally determined, in the same ranges of m and w . It is last to compare the PC + DEC solution of LiBF₄ with that of LiPF₆ for their T_g and κ and to explain the observed similarities and differences.

Experimental Section

PC of 99.98% purity and DEC of 99.95% purchased from Grant Chemical, and LiBF₄ of 99.9% from Stella Chemifa, were used without further treatment. In an argon-filled drybox, PC and DEC were mixed to form seven mixtures,

* To whom correspondence may be addressed. E-mail: mding@arl.army.mil.

Table 1. Measured Values of Electrolytic Conductivity κ of $\text{LiBF}_4(m) + (1 - w)\text{PC} + w\text{DEC}$ Solution at Different Molalities m , Mass Fractions w , and Temperatures θ , and Glass Transition Temperatures T_g at the Same Values of m and w

$m/(\text{mol kg}^{-1})$	T_g/K	$\kappa/(\mu\text{S cm}^{-1})$ at the following θ ($^{\circ}\text{C}$)														
		59.0	49.2	39.3	29.4	19.5	9.7	-0.2	-10.0	-19.8	-29.5	-39.4	-49.3	-59.2	-69.0	-79.0
$w = 0.0000$																
2.3579	191.7	3391	2674	2043	1502	1055	691.8	415.3	222.6	101.9	37.63	10.37	1.811	0.1714	0.005676	
2.1245	188.7	3806	3049	2370	1775	1277	862.2	537.6	302.2	146.9	58.94	17.92	3.603	0.4168	0.02072	
1.8555	185.2	4343	3536	2803	2146	1584	1105	717.8	424.1	220.5	96.40	32.95	7.754	1.108	0.07576	
1.6678	182.5	4756	3915	3139	2444	1836	1307	871.4	532.9	289.3	133.9	49.38	12.88	2.110	0.1748	0.004917
1.5020	180.0	5077	4269	3461	2726	2080	1507	1028	647.4	364.5	177.1	69.57	19.79	3.641	0.3536	0.01291
1.3582	178.6	5470	4581	3753	2986	2305	1699	1179	759.8	441.2	222.7	92.30	28.14	5.652	0.6155	0.02799
1.1987		5839	4932	4078	3283	2568	1923	1362	899.4	538.5	284.0	124.3	40.96	9.110	1.155	0.06336
1.0634	174.5	6130	5216	4348	3533	2791	2117	1524	1026	631.0	344.2	157.6	55.27	13.43	1.877	0.1192
0.9507	172.8	6342	5427	4550	3727	2968	2277	1657	1134	712.2	399.0	189.4	69.75	18.05	2.753	0.1955
0.8373	171.0	6516	5608	4731	3900	3134	2425	1789	1243	795.8	457.3	224.8	86.84	23.96	3.961	0.3136
0.7375	169.6	6613	5716	4848	4020	3254	2537	1889	1328	863.7	507.7	257.5	103.3	30.06	5.337	0.4632
0.6499	168.0	6639	5761	4905	4088	3327	2613	1965	1397	921.7	551.1	285.5	118.6	36.07	6.816	0.6386
0.5602	167.4	6589	5738	4907	4110	3365	2660	2016	1449	968.8	589.7	313.1	134.5	42.87	8.606	0.8695
0.4751	166.2	6441	5628	4834	4063	3342	2660	2030	1473	998.1	617.0	334.7	148.2	49.20	10.45	1.143
0.3762	165.0	6099	5348	4607	3893	3216	2578	1987	1454	999.5	628.5	349.6	160.0	56.03	12.66	1.496
0.2863	163.9	5560	4891	4230	3588	2976	2399	1862	1376	955.2	611.1	347.1	164.0	59.37	14.24	1.813
0.0000	160.5															
$w = 0.1002$																
2.1787	186.0	3747	3022	2373	1801	1315	904.2	576.9	334.1	169.7	72.07	24.00	5.427	0.7276	0.04400	
1.9754	183.0	4122	3368	2680	2063	1534	1080	709.4	426.0	226.5	102.6	36.90	9.277	1.456	0.1120	
1.7262	180.6	4618	3826	3093	2426	1844	1333	904.8	566.2	317.9	154.5	61.10	17.52	3.271	0.3219	0.01184
1.5531	177.6	4981	4164	3402	2703	2085	1532	1062	683.3	397.1	202.1	84.87	26.46	5.545	0.6387	0.03063
1.3968	176.0	5261	4481	3693	2965	2316	1727	1222	805.3	482.0	255.1	112.9	37.86	8.744	1.153	0.06824
1.2546	174.0	5613	4764	3964	3213	2535	1918	1377	926.0	569.3	311.4	144.1	51.38	12.83	1.871	0.1302
1.1095	172.1	5900	5044	4230	3460	2760	2116	1543	1058	666.8	377.4	182.4	69.14	18.77	3.118	0.2508
0.9830	169.8	6121	5264	4443	3662	2945	2283	1687	1176	757.1	440.6	220.9	88.07	25.64	4.641	0.4233
0.8770	168.4	6269	5420	4597	3816	3088	2416	1803	1273	833.7	495.8	256.0	106.2	32.71	6.377	0.6401
0.7770	166.9	6367	5529	4713	3932	3208	2525	1905	1360	904.5	548.3	290.4	125.2	40.44	8.403	0.9267
0.6801	165.7	6404	5586	4782	4009	3291	2608	1982	1430	964.0	595.7	324.0	144.0	48.66	10.76	1.291
0.5968	164.7	6374	5575	4791	4035	3327	2654	2034	1482	1010	632.8	350.3	160.1	56.26	13.14	1.686
0.5137	163.9	6270	5501	4744	4011	3324	2665	2056	1511	1042	662.4	373.9	175.6	64.01	15.69	2.159
0.4349	162.8	6075	5346	4626	3924	3257	2634	2043	1514	1053	678.2	389.5	187.4	70.56	18.15	2.667
0.3563	161.9	5760	5082	4407	3752	3129	2538	1983	1478	1041	677.0	395.6	194.7	76.04	20.39	3.172
0.2981	161.5	5409	4782	4159	3548	2966	2413	1892	1419	1003	659.6	389.8	195.8	77.74	21.65	3.513
0.0000	158.1															
$w = 0.2006$																
2.0632	181.0	3923	3220	2582	2008	1510	1077	720.7	443.7	244.0	115.6	44.37	12.30	2.173	0.1957	0.005771
1.8700		4265	3541	2872	2261	1727	1257	861.1	546.0	312.0	155.6	63.83	19.30	3.895	0.4268	0.01795
1.6613	176.5	4648	3900	3197	2557	1984	1473	1034	675.8	401.8	210.8	92.62	30.82	7.092	0.9307	0.05411
1.4946	175.4	4962	4196	3477	2808	2207	1662	1189	795.0	486.5	265.4	122.6	43.85	11.13	1.676	0.1191
1.3424	171.5	5200	4470	3732	3042	2418	1844	1341	915.9	574.8	324.0	156.6	59.59	16.45	2.788	0.2333
1.2080		5485	4700	3956	3250	2607	2012	1482	1029	660.4	382.4	191.6	76.62	22.59	4.171	0.4020
1.0728	167.9	5703	4918	4167	3451	2793	2179	1626	1147	750.9	447.3	232.4	97.64	30.86	6.354	0.6919
0.9624	165.9	5856	5074	4320	3600	2932	2307	1740	1243	827.7	503.6	268.6	117.5	39.09	8.633	1.042
0.8610	164.8	5960	5190	4438	3720	3045	2417	1838	1328	896.6	555.6	304.0	137.3	47.99	11.29	1.485
0.7770	163.6	6021	5262	4522	3807	3139	2505	1921	1402	959.0	604.1	337.7	157.5	57.38	14.25	2.035
0.6801	162.5	6027	5290	4563	3860	3200	2569	1984	1462	1012	648.3	370.8	178.0	67.42	17.71	2.735
0.5968	161.0	5972	5256	4549	3865	3216	2598	2021	1502	1050	681.1	395.5	194.2	76.15	21.00	3.443
0.4992	160.7	5844	5158	4479	3819	3196	2593	2030	1520	1075	706.2	417.5	210.2	85.04	24.49	4.296
0.4162	160.7	5620	4974	4334	3707	3112	2541	2000	1509	1075	715.3	429.8	221.1	92.24	27.81	5.178
0.3416	158.4	5308	4708	4111	3528	2968	2434	1927	1462	1055	706.6	430.6	225.9	96.86	30.12	5.918
0.2723		4881	4339	3799	3268	2757	2269	1803	1377	996.0	675.3	416.5	222.9	97.57	31.63	6.467
0.0000	154.6															
$w = 0.2999$																
2.0606	178.3	3848	3194	2596	2053	1574	1151	794.1	508.8	294.7	149.9	63.01	19.98	4.272	0.5005	0.02359
1.8826	175.1	4128	3460	2838	2267	1761	1308	920.4	604.5	361.4	191.4	85.24	29.01	6.894	0.9480	0.05718
1.6841	175.0	4443	3759	3114	2521	1985	1500	1077	725.8	448.5	247.9	116.9	43.11	11.46	1.842	0.1421
1.5154	171.6	4715	4019	3361	2745	2187	1675	1223	840.9	533.5	305.0	150.4	59.05	17.17	3.130	0.2899
1.3648	169.4	4914	4249	3578	2947	2372	1837	1361	953.1	618.0	363.7	186.5	77.45	24.20	4.889	0.5254
1.2292	168.4	5150	4442	3769	3127	2538	1987	1490	1059	700.2	422.3	223.5	96.84	32.11	7.047	0.8609
1.0960	166.5	5324	4620	3944	3296	2696	2131	1616	1164	784.4	484.3	264.8	119.9	42.20	10.17	1.390
0.9828	163.0	5447	4749	4071	3423	2816	2244	1719	1253	856.2	539.2	301.8	141.5	52.25	13.43	2.019
0.8762	161.8	5528	4842	4171	3525	2915	2342	1809	1333	922.5	590.4	338.2	163.6	63.07	17.21	2.808
0.7708	160.6	5568	4897	4238	3598	2996	2420	1884	1402	982.9	639.8	374.2	186.4	74.92	21.51	3.805
0.6770	159.0	5555	4903	4257	3631	3038	2467	1932	1451	1027	678.2	404.4	206.4	85.78	25.88	4.892
0.5943	158.4	5492	4859	4234	3625	3044	2486	1960	1481	1060	707.4	427.4	222.7	95.24	29.97	5.998
0.5049	157.1	5357	4754	4156	3571	3013	2472	1961	1493	1079	729.1	448.0	238.7	105.0	34.43	

Table 1 (Continued)

$m/(\text{mol kg}^{-1})$	T_g/K	$\kappa/(\mu\text{S cm}^{-1})$ at the following θ ($^{\circ}\text{C}$)														
		59.0	49.2	39.3	29.4	19.5	9.7	-0.2	-10.0	-19.8	-29.5	-39.4	-49.3	-59.2	-69.0	-79.0
$w = 0.4000$																
2.0559	3664	3073	2529	2030	1583	1184	839.8	557.7	338.7	183.6	84.36	29.93	7.694	1.167	0.08274	
1.8735	3904	3305	2743	2222	1755	1331	960.7	652.6	407.7	229.0	110.5	42.24	11.83	2.069	0.1798	
1.6793	4159	3550	2974	2436	1947	1499	1102	764.3	491.2	286.0	144.7	59.25	18.24	3.642	0.3863	
1.5080	4378	3765	3181	2627	2123	1654	1233	871.8	573.2	343.9	181.1	78.25	26.04	5.806	0.7240	
1.3659	4524	3936	3344	2784	2268	1785	1348	966.6	647.1	397.4	216.3	97.72	34.46	8.365	1.171	
1.2363	4694	4078	3487	2921	2397	1903	1452	1055	717.8	450.1	251.0	117.4	43.52	11.29	1.771	
1.0955	4824	4214	3625	3056	2527	2025	1561	1148	795.0	508.9	292.5	142.4	55.67	15.70	2.732	
0.9833	4903	4302	3731	3150	2618	2112	1643	1221	855.8	557.4	326.9	163.9	66.80	19.94	3.766	
0.8778	4946	4357	3780	3219	2688	2185	1713	1285	911.1	601.6	360.0	185.4	78.40	24.62	4.991	
0.7783	4952	4379	3813	3263	2740	2237	1765	1336	956.9	641.1	390.1	205.9	90.04	29.46	6.389	
0.6897	4922	4366	3812	3275	2762	2265	1796	1370	989.2	670.8	414.9	223.4	100.4	34.28	7.833	
0.6082	4853	4313	3780	3259	2756	2273	1814	1391	1015	694.5	434.4	238.2	109.7	38.80	9.309	
0.5237	4731	4218	3706	3204	2723	2254	1808	1397	1027	709.9	450.5	251.7	118.7	43.40	10.95	
0.4421	4548	4066	3583	3106	2642	2203	1775	1380	1021	713.0	457.0	260.3	125.6	47.41	12.52	
0.3618	4286	3841	3392	2952	2521	2106	1703	1334	996.1	700.6	455.2	262.8	129.6	50.31	13.92	
0.2828	3920	3518	3117	2718	2332	1951	1587	1248	936.6	665.7	437.3	256.9	129.1	51.78	14.81	
$w = 0.5000$																
2.0516	3406	2888	2405	1957	1554	1187	865.7	595.1	378.2	217.7	108.5	43.39	13.16	2.547	0.2566	
1.8636	3596	3077	2584	2122	1703	1319	976.9	685.7	446.8	265.3	138.1	58.83	19.26	4.216	0.5066	
1.6539	3806	3280	2780	2308	1875	1472	1109	793.8	531.2	326.0	177.2	80.42	28.67	7.089	1.023	
1.5009	3945	3421	2917	2440	1998	1583	1207	876.2	596.7	374.6	209.9	99.15	37.43	10.05	1.639	
1.3570	4041	3540	3037	2557	2109	1687	1299	956.1	661.2	423.6	244.2	119.7	47.51	13.71	2.470	
1.2239	4152	3635	3136	2656	2206	1778	1382	1028	721.7	471.0	277.2	140.1	57.95	17.75	3.522	
1.0935	4217	3712	3215	2740	2290	1859	1458	1096	779.5	517.1	312.0	162.8	70.23	22.89	4.943	
0.9834	4248	3754	3265	2795	2347	1918	1515	1148	825.7	555.9	340.9	182.1	81.41	27.81	6.411	
0.8815	4254	3785	3292	2828	2386	1962	1561	1193	865.7	587.9	367.8	200.7	92.43	32.9	8.041	
0.7819	4228	3759	3297	2843	2409	1989	1591	1226	897.1	618.8	391.5	217.5	103.4	38.18	9.867	
0.6906	4172	3719	3271	2825	2408	1997	1605	1245	920.0	640.6	410.8	233.4	113.3	43.34	11.73	
0.6132	4092	3668	3225	2800	2388	1990	1607	1252	932.0	654.6	424.2	244.5	120.8	47.58	13.41	
0.5316	3971	3559	3147	2743	2347	1961	1592	1245	934.7	662.1	434.4	254.1	128.2	51.90	15.23	
0.4503	3803	3416	3029	2644	2275	1906	1555	1214	923.7	660.3	437.7	259.9	133.8	55.69	16.96	
0.3689	3569	3206	2856	2503	2155	1815	1485	1179	895.1	644.6	431.8	260.1	136.3	58.20	18.49	
0.2901	3254	2938	2615	2297	1985	1676	1379	1098	838.2	608.2	411.2	251.6	134.3	58.82	19.24	
$w = 0.5997$																
2.0508	3061	2622	2210	1825	1473	1148	858.2	608.8	403.1	244.7	131.3	58.45	20.50	4.942	0.6865	
1.8736	3188	2751	2335	1942	1582	1248	945.3	682.1	461.0	286.9	159.5	74.46	27.81	7.380	1.177	
1.6658	3323	2887	2471	2076	1709	1364	1048	769.9	532.2	340.8	196.2	96.64	38.71	11.36	2.109	
1.5116	3406	2976	2561	2166	1797	1446	1123	835.1	586.1	382.6	226.1	115.2	48.40	15.22	3.128	
1.3701	3451	3042	2632	2239	1869	1516	1188	893.7	635.6	422.3	255.4	134.2	58.75	19.60	4.383	
1.2344	3503	3089	2685	2298	1929	1576	1246	946.2	681.8	460.1	283.4	152.8	69.29	24.32	5.879	
1.0932	3517	3117	2723	2342	1979	1628	1298	995.2	725.8	497.4	313.2	173.9	81.89	30.35	7.933	
0.9801	3506	3117	2734	2361	2004	1658	1330	1028	757.0	525.4	335.9	190.1	92.36	35.62	9.834	
0.8744	3469	3095	2724	2361	2011	1674	1352	1052	781.5	547.9	355.4	205.2	102.2	40.83	11.86	
0.7693	3403	3045	2690	2341	2004	1674	1358	1065	797.9	565.9	371.8	218.6	111.6	46.11	14.04	
0.6766	3316	2976	2637	2300	1976	1658	1351	1066	803.5	575.7	382.7	228.7	119.2	50.67	16.05	
0.5945	3210	2887	2564	2244	1934	1629	1334	1057	803.2	579.3	388.8	235.5	124.6	54.36	17.85	
0.5114	3070	2768	2465	2163	1871	1580	1300	1036	791.5	575.4	390.4	239.4	129.2	57.66	19.60	
0.4230	2875	2598	2320	2043	1772	1502	1242	994.4	765.2	560.9	384.4	239.1	131.4	60.30	21.16	
0.3448	2652	2403	2151	1899	1650	1405	1164	939.2	725.8	535.8	370.4	233.2	130.1	60.91	22.11	
0.2652	2361	2144	1924	1702	1484	1265	1055	852.5	663.6	492.8	344.0	219.4	124.5	59.53	22.19	
$w = 0.6998$																
2.0444	2597	2249	1919	1608	1319	1049	804.3	588.6	405.3	258.8	148.7	72.87	29.19	8.609	1.609	
1.8613	2664	2324	1996	1684	1394	1120	869.3	645.8	453.0	295.6	175.1	89.40	37.85	12.08	2.531	
1.6253	2725	2395	2075	1767	1478	1203	946.6	715.6	512.7	343.9	210.5	112.9	50.98	17.82	4.283	
1.4939	2741	2421	2106	1803	1517	1242	985.0	751.3	544.6	370.2	230.9	126.8	59.08	21.67	5.581	
1.3536	2734	2433	2127	1829	1548	1276	1020	785.4	575.5	397.1	252.4	142.1	68.46	26.27	7.239	
1.2046	2725	2425	2130	1843	1568	1302	1048	814.9	604.3	422.9	273.3	157.4	78.26	31.40	9.249	
1.0486	2675	2392	2111	1836	1571	1313	1066	836.6	627.4	445.5	293.6	173.7	89.28	37.59	11.84	
0.9229	2606	2338	2072	1810	1556	1307	1068	844.4	638.7	458.9	306.7	184.6	97.53	42.49	14.05	
0.8102	2518	2267	2016	1767	1524	1287	1058	841.7	642.1	465.4	315.1	193.0	104.1	46.75	16.13	
0.7018	2407	2173	1938	1705	1478	1253	1034	827.8	636.3	465.7	318.7	198.2	109.2	50.39	18.05	
0.6106	2288	2071	1852	1633	1419	1208	1001	805.2	622.2	459.5	317.3	200.0	112.1	52.91	19.53	
0.5302	2160	1959	1756	1553	1353	1156	961.6	776.9	604.1	448.5	312.5	199.0	112.7	54.35	20.62	
0.4472	2002	1819	1635	1449	1268	1085	906.6	735.9	575.3	429.9	302.4	194.6	112.2	55.06	21.52	
0.3561	1791	1632	1470	1307	1147	984.9	827.2	674.1	530.4	399.5	283.4	184.7	108.2	54.50	21.80	
0.2824	1582	1445	1305	1162	1022	880.8	741.1	608.4	479.7	363.7	260.0	171.1	101.6	51.86	21.35	
0.2029	1312	1201	1087	971.5	856.5	739.4	625.5	514.1	408.9	311.3	224.7	149.5	90.14	46.90	19.78	

in addition to pure PC, in mass fractions w of DEC from 0.1 to 0.7 in 0.1 increments, from which eight electrolytes were subsequently made by dissolving LiPF_6 into each of the solvents to a molality m of around 2.1 mol kg^{-1} .

Conductivity measurements on these solutions and their subsequent dilution for the next set of less concentrated solutions were done in a dry room. At the end of each measurement,

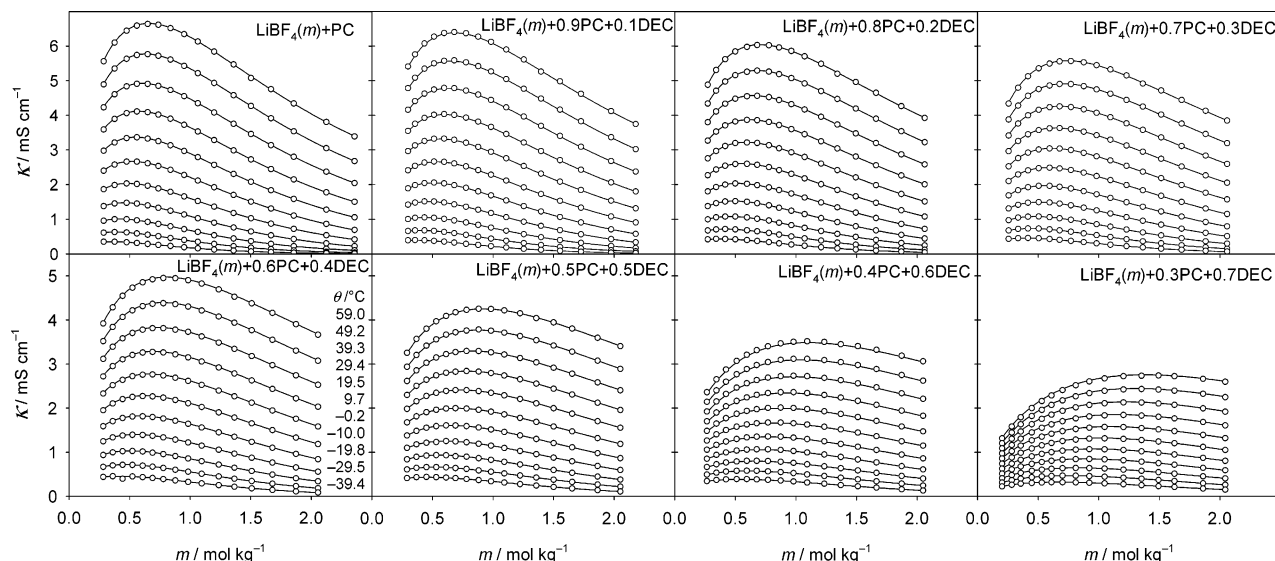


Figure 1. Change of conductivity κ with salt molality m at different temperatures θ and solvent mass fractions w for $\text{LiBF}_4(m) + (1-w)\text{PC} + w\text{DEC}$ solution. The open circles represent measured data, and the curves plot their fitting functions of eqs 1 and 2.

each electrolyte for the determination of its glass transition temperature.¹

Conductivity κ of the electrolytes was measured with an HP (now Agilent) 4284A precision LCR meter at selected temperatures within a Tenney Jr. Environmental Chamber, controlled and coordinated with a house-made computer program.^{1,8} The conductivity cells consisted of a pair of platinum–iridium electrodes and a Pyrex cell body with a nominal cell constant of 0.1 cm^{-1} . Temperature θ of the measurements went from (60 to -80) °C in 10-K decrement, stopping at each for an hour of thermal equilibration before a measurement. The measurement consisted of an impedance scan from 1 MHz to 20 Hz with an amplitude of 10 mV, from which a ZZ' plot was made and κ was evaluated from the impedance curve, with an overall uncertainty of 0.5% in the measurement. More details on the estimation of the measurement uncertainty and on the evaluation of electrolyte resistance from the impedance curve can be found in ref 1.

A modulated differential scanning calorimeter (MDSC 2920, TA Instruments) cooled with liquid nitrogen was used to determine the glass transition temperature T_g of a sample. Vitrification of the sample was achieved by dipping into liquid nitrogen a small amount of sample crimp sealed in a pair of aluminum pans and lids (0219-0062, Perkin-Elmer Instruments). The sample was then quickly placed onto the differential scanning calorimeter sample stage that had been kept at a temperature below the T_g of the sample. A modulated heating schedule was then applied, with a heating rate of 2 K/min and a modulation of 60-s period and 0.5-K amplitude. T_g was subsequently determined for the sample on the reversing component of the heat flow at the inflection point of the endothermic step associated with the glass transition.^{1,8} The uncertainty in the T_g values thus determined was estimated to be 0.5 K.

Results and Discussion

As will be shown, change of κ with m , w , and θ of the electrolyte system $\text{LiBF}_4(m) + (1-w)\text{PC} + w\text{DEC}$ can be consistently explained with the changes of ϵ of the solvent and the η of the solvent and the solution with the same variables. Thus, ϵ and η of the $\text{PC}_{1-w}\text{DEC}_w$ binary solvent have been systematically studied and were both found to fall monotonically and smoothly with w and with θ .⁷ This

is exactly what one would expect knowing the values of the end members (ϵ values of PC and DEC at 40 °C are 61.43 and 2.809, and η values are 1.91 mPa s and 0.622 mPa s, respectively)²⁴ and the normal ways ϵ and η of a binary solvent of similar components change with their relative proportions and with θ .^{5–13}

Change of Conductivity with Salt Content, Solvent Composition, and Temperature. Results of the κ measurement in the range of (-80 to 60) °C for the $\text{LiBF}_4(m) + (1-w)\text{PC} + w\text{DEC}$ electrolyte are tabulated in Table 1, of which the part from (60 to -40) °C is also plotted in Figure 1 as eight κm plots with the open circles representing the measured data and the curves plotting their fitting functions $\kappa = f(m, w)$ at the particular temperatures. These functions were obtained by extending the Casteel–Amis equation³⁶ to include w as an additional variable by setting the equation parameters to polynomial functions of w . That is

$$\kappa = m^a \exp(b + cm + dm^2) \quad (1)$$

where a , b , c , and d are third-degree polynomials of w

$$p = p_0 + p_1 w + p_2 w^2 + p_3 w^3 \quad (2)$$

with p standing for a , b , c , or d . Use of eq 1 as the basic form for the fitting functions was due to its ability to faithfully describe the dependency of κ on m in wide ranges of m as shown in Figure 1 and in many other studies,^{15,24,28,29,38} which was found difficult to achieve with a polynomial function. The choice for the degree of the polynomial of eq 2, on the other hand, was based on its use in eq 1 resulting in the best fit to the measured data. Thus, the bivariate function of eq 1 was fitted to the κ –(m, w) data for each θ from (60 to -40) °C for the determination of its parameters, with an average fitting error of 0.46% of the data range. These fitted functions are plotted in Figure 1 with the corresponding experimental data to demonstrate the closeness of the fit and in Figure 2 as κ surfaces in $m w$ coordinates to show the change of κ with simultaneous changes of m and w and with θ .

The κ surfaces as shown in Figure 2 reveal a number of interesting features, the most conspicuous of which is the “dome” shape they assume in the $m w$ coordinates as a result of κ peaking in both m and w . Peaking of κ in m is

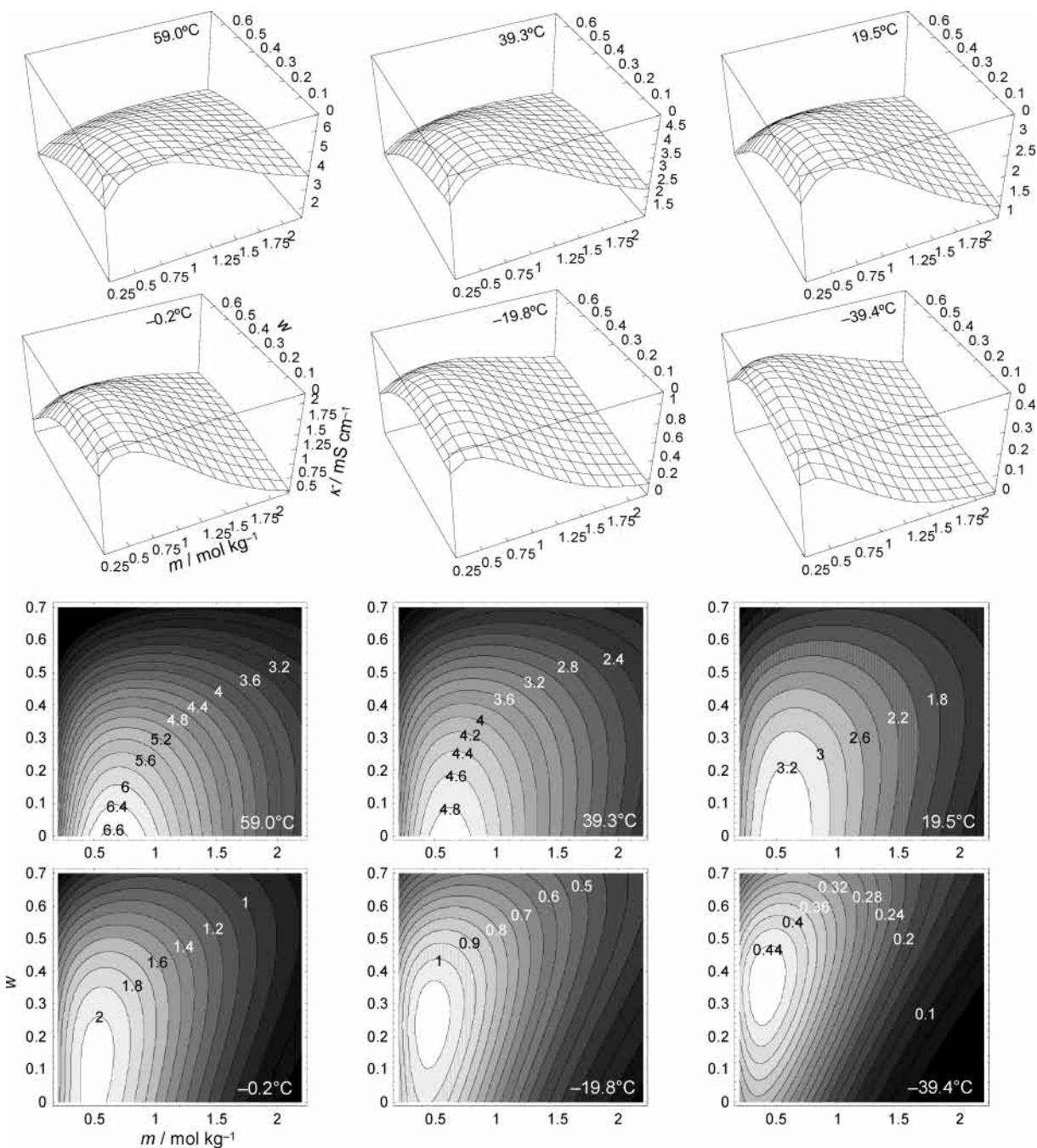


Figure 2. Change of conductivity κ with simultaneous changes in salt molality m and solvent mass fraction w for $\text{LiBF}_4(m) + (1 - w)\text{PC} + w\text{DEC}$ solution according to eqs 1 and 2 that have been fitted to the measured $\kappa(m, w)$ data. Each function is doubly represented by a surface plot (upper plots) and a contour plot (lower plots) with the temperature and the contour values indicated in the plots.

a common feature for liquid electrolytes, reflecting the process of κ first increasing with the dissociated ion number as m increases and then falling as the rise of η and of ion association become dominant; this has been observed for many electrolytes of lithium salts.^{8,15,24,25,28–30,36,38} The peaking of κ in w , on the other hand, seems to be the result of the ϵ and η values of DEC both being much lower than those of PC and of the mixture both being monotonic functions of w . As such, as w rises from zero, the change of κ is first dominated by the fall of η of the electrolyte causing κ to rise and then by the fall of ϵ of the solvent which by allowing stronger ion association causes κ to fall. The same behavior has been observed in $\text{LiPF}_6 + \text{PC} + \text{DEC}$,^{1,26} $\text{LiPF}_6 + \text{EC} + \text{EMC}$,²⁵ $\text{LiClO}_4 + \text{PC} + \text{DME}$,¹¹ and $\text{NaClO}_4 + \text{PC} + \text{DME}$,¹² where DEC, EMC, and DME have

much lower ϵ and η values than PC, EC, and PC, respectively.

Another feature of Figure 2 is the shifting of the κ dome in the direction of low m and high w as θ lowers. This is the result of θ affecting the dome-forming process discussed above. As η rises with lowering θ , the peaking of κ with rising m would occur earlier as the higher η helps to offset the increase in the dissociated ion number. By the same token, the peaking of κ with rising w occurs later as the higher η delays the dominance of ion association over a falling η . The rapid rise of η with falling θ also explains the general fall in height of the domes shown in Figure 2. In addition, as θ lowers, the dome becomes narrower in the direction of m , indicating an increase in the rate with which η rises with m at lower θ . All of these features have

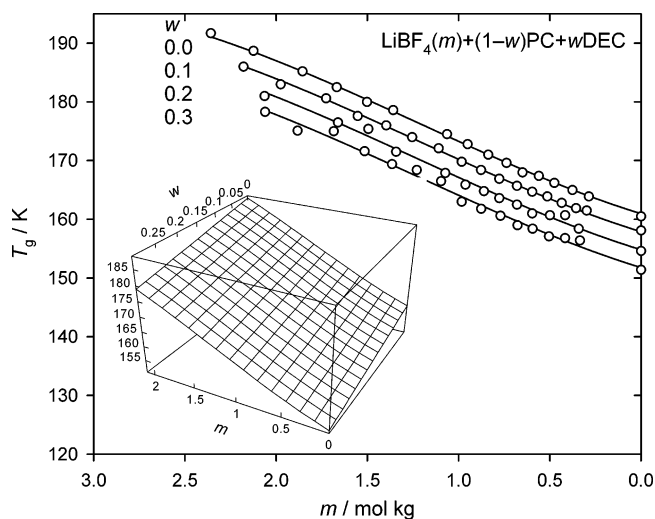


Figure 3. Change of glass transition temperature T_g with salt molality m and solvent mass fraction w for $\text{LiBF}_4(m) + (1-w)\text{PC} + w\text{DEC}$ solution. The open circles represent the measured data, and the curves plot their fitting function of eq 3, which is also plotted as a 3D surface as inserted in the figure.

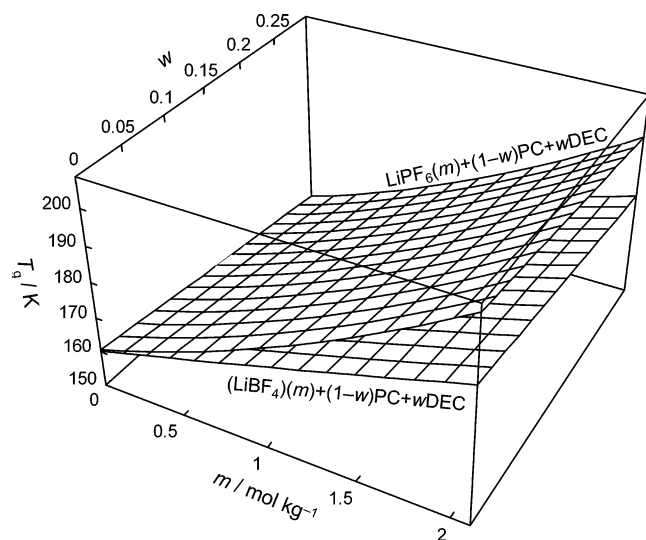


Figure 4. Comparison of T_g surfaces in the coordinates of salt molality m and solvent mass fraction w for the electrolytes $\text{LiBF}_4(m) + (1-w)\text{PC} + w\text{DEC}$ (from Figure 3) and $\text{LiPF}_6(m) + (1-w)\text{PC} + w\text{DEC}$ (from ref 1), as indications for the changes in their viscosities.

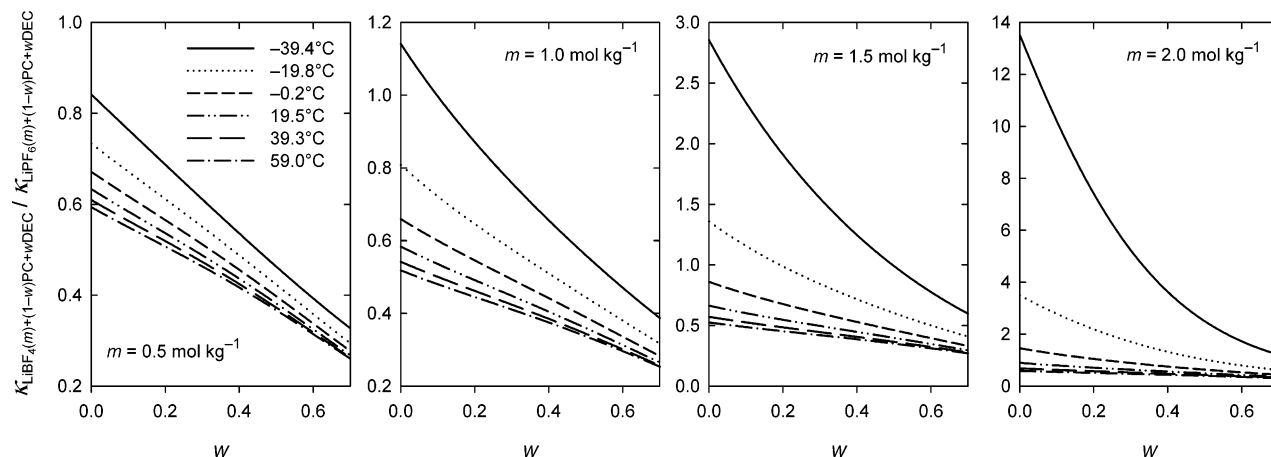


Figure 5. Change with solvent mass fraction w of the ratio in κ of the $(1-w)\text{PC} + w\text{DEC}$ solution of LiBF_4 (from Figure 2) over that of LiPF_6 (from ref 1) at different salt molalities m and temperatures, as indicated in the plots.

been observed in $\text{LiPF}_6 + \text{PC} + \text{DEC}$ and $\text{LiPF}_6 + \text{EC} + \text{EMC}$ solutions as described previously.^{1,25,26}

Change of Glass Transition Temperature with Salt Content and Solvent Composition. Results of the T_g measurement for the $\text{LiBF}_4(m) + (1-w)\text{PC} + w\text{DEC}$ electrolyte are tabulated in Table 1 and plotted in Figure 3 with the open circles for the measured data and the curves for their fitting function

$$T_g/K = 160.96 + 9.542m + 3.8182m^2 - 1.0393m^3 - 30.633w \quad (3)$$

where m is the salt concentration in mol kg^{-1} , w the mass fraction of DEC, the application range is (0 to 2.1) for m and (0 to 0.3) for w , and the fitting error is 1.3% of the data range. This equation is also plotted as a T_g surface in the mw coordinates as the insert in the figure, describing a simple surface slanting down from the corner of high m and low w toward that of low m and high w . This change of T_g , when viewed as a reflection of change in η ,⁷ is entirely consistent with the change of κ with m , w , and θ as has just been discussed. It also seems that the rise of T_g due to the addition of salt was independent of that due to the change of solvent composition. This can be seen in the shape of the T_g surface and the curves and above all in the absence of a cross-product term in the fitting function of eq 3.

Comparison of LiBF_4 with LiPF_6 for Their T_g and κ . In Figure 4 are plotted together the T_g surfaces of $\text{LiBF}_4(m) + (1-w)\text{PC} + w\text{DEC}$ of Figure 3 and of $\text{LiPF}_6(m) + (1-w)\text{PC} + w\text{DEC}$ of ref 1, which shows the T_g of LiBF_4 being consistently lower than that of LiPF_6 , with the difference increasing with higher m and lower w . This indicates that, although both salts raise the η of the electrolytes, the effect is considerably stronger for LiPF_6 than LiBF_4 . This is most likely the result of a stronger ion association of BF_4^- than PF_6^- with Li^+ in the electrolytes due to the smaller size of BF_4^- , which leaves fewer free Li^+ in the solvent for binding to the solvent molecules via solvation and thereby raising the η of the electrolyte. By this mechanism, the disparity in η between the two salts would increase with higher m and lower w , as is indeed seen in Figure 4.

The lower η of LiBF_4 than LiPF_6 also explains the differences in κ of the two salts in the same solvent $\text{PC} + \text{DEC}$, as shown in Figure 5 where the ratio in κ of LiBF_4 in $\text{PC} + \text{DEC}$ over LiPF_6 in the same solvent is plotted as a function of solvent composition at four different salt

concentrations. As can be seen, at a low m value of 0.5 mol kg⁻¹, where η of the electrolytes is relatively low, the ratio is below unity at all values of θ , though it grows larger with lower θ and w . This is because, when η is low, ion pairing plays a dominant role in determining the κ of the electrolytes, which is always stronger for LiBF₄ than for LiPF₆. However, this dominance gets weaker as the η becomes higher at lower θ and w , where the lower η of LiBF₄ solution starts to assert its influence and cause its κ to rise relative to that of LiPF₆. This trend continues as m becomes higher, accompanied by a higher η , as shown in Figure 5 from left to right. At 1.0 mol kg⁻¹ of m , for example, the ratio of κ is already above unity at -39.4 °C when w is below 0.1. The same occurs at -19.8 °C when w is below 0.5 and m is increased to 1.5 mol kg⁻¹. At a high value of 2.0 mol kg⁻¹ of m , the lower η of LiBF₄ becomes so dominant over its stronger ion association that its κ rises over that of LiPF₆ by more than 10 times at -39.4 °C and low values of w .

Conclusions

Electrolytic conductivity κ of the electrolyte system LiBF₄(m) + (1 - w)PC + w DEC was measured and tabulated in the ranges of salt molality m , solvent mass fraction w , and temperature θ of (0.2 to 2.1) mol kg⁻¹, (0 to 0.7), and (-80 to 60) °C, respectively, with an uncertainty of 0.5%. Its glass transition temperature T_g was also measured and tabulated in the same ranges of m and w , with an uncertainty of 0.5 K. The κ in its change with m and w peaked in both variables and thus formed a "dome" when plotted as a 3D surface in the mw coordinates, as a result of PC having a dielectric constant ϵ and a viscosity η much higher than those of DEC. In addition, as θ was lowered, the κ surfaces fell in height and shifted in the direction of lower η . The T_g of the electrolyte rose with m and fell with w , the effects of m and w being largely independent of each other. These results, when compared to those of LiPF₆ in the same solvent, showed that the T_g of the LiBF₄ solution was lower than that of the LiPF₆, indicating a lower η value of the former, and the κ was generally lower because of the stronger ion association of Li⁺ with BF₄⁻ than with PF₆⁻, except at high m and low θ , where the lower η value of the LiBF₄ solution made it more conductive.

Literature Cited

- Ding, M. S. Electrolytic Conductivity and Glass Transition Temperature as Functions of Salt Content, Solvent Composition, or Temperature for LiPF₆ in Propylene Carbonate + Diethyl Carbonate. *J. Chem. Eng. Data* **2003**, *48*, 519–528.
- Ding, M. S.; Jow, T. R. How Conductivities of PC-DEC and PC-EC Solutions of LiBF₄, LiPF₆, LiBOB, Et₄NBF₄, and Et₄NPF₆ Differ and Why. *J. Electrochem. Soc.*, in press.
- Jow, T. R.; Ding, M. S.; Xu, K.; Zhang S. S.; Allen, J. L.; Amine, K.; Henriksen, G. L. Nonaqueous Electrolytes for Wide-Temperature-Range Operation of Li-Ion Cells. *J. Power Sources* **2003**, *119*, 343–348.
- Ding, M. S. Liquid-Solid-Phase Equilibria and Thermodynamic Modeling for Binary Organic Carbonates. *J. Chem. Eng. Data* **2004**, *49*, 276–282.
- Electrolyte Data Collection, Part 2a, Dielectric Properties of Nonaqueous Electrolyte Solutions*; Barthel, J., Buchner, R., Munsterer, M., Eds.; DECHEMA: Frankfurt, 1996; Chemistry Data Series, Vol. XII.
- Barthel, J.; Neueder, R.; Roch, H. Density, Relative Permittivity, and Viscosity of Propylene Carbonate + Dimethoxyethane Mixtures from 25 °C to 125 °C. *J. Chem. Eng. Data* **2000**, *45*, 1007–1011.
- Ding, M. S. Liquid-Phase Boundaries, Dielectric Constant, and Viscosity of PC-DEC and PC-EC Binary Carbonates. *J. Electrochem. Soc.* **2003**, *150*, A455–A462.
- Ding, M. S.; Xu, K.; Jow, T. R. Effects of Tris(2,2,2-trifluoroethyl) Phosphate as a Flame-Retarding Cosolvent on Physicochemical Properties of Electrolytes of LiPF₆ in EC-PC-EMC of 3:3:4 Weight Ratios. *J. Electrochem. Soc.* **2002**, *149*, A1489–A1498.
- Blomgren, G. E. Properties, Structure and Conductivity of Organic and Inorganic Electrolytes for Lithium Battery Systems. In *Lithium Batteries*; Gabano, J.-P., Ed.; Academic Press: London, 1983.
- Matsuda, Y.; Morita, M.; Yamashita, T. Conductivity of the LiBF₄/Mixed Ether Electrolytes for Secondary Lithium Cells. *J. Electrochem. Soc.* **1984**, *131*, 2821–2827.
- Matsuda, Y.; Morita, M.; Kosaka, K. Conductivity of the Mixed Organic Electrolyte Containing Propylene Carbonate and 1,2-Dimethoxyethane. *J. Electrochem. Soc.* **1983**, *130*, 101–104.
- Matsuda, Y.; Satake, H. Mixed Electrolyte Solutions of Propylene Carbonate and Dimethoxyethane for High Energy Density Batteries. *J. Electrochem. Soc.* **1980**, *127*, 877–879.
- Payne, R.; Theodorou, I. E. Dielectric Properties and Relaxation in Ethylene Carbonate and Propylene Carbonate. *J. Phys. Chem.* **1972**, *76*, 2892–2900.
- Electrolyte Data Collection, Parts 3a and 3b, Viscosity of Non-Aqueous Solutions II: Aprotic and Protic Non-Alcohol Solutions C₁-C₃ and C₄-C₈*; Barthel, J., Neueder, R., Meier, R., Eds.; DECHEMA: Frankfurt, 2000; Chemistry Data Series, Vol. XII.
- Cisak, A.; Werblan, L. *High-Energy Nonaqueous Batteries*; Ellis Horwood: New York, 1993; Chapter 7.
- Casteel, J. F.; Angel, J. R.; McNeeley, H. B.; Sears, P. G. Conductivity-Viscosity Studies on Some Moderately Concentrated Nonaqueous Electrolyte Solutions from -50° to 125°. *J. Electrochem. Soc.* **1975**, *122*, 321–324.
- Petrella, G.; Sacco, A. Viscosity and Conductance Studies in Ethylene Carbonate at 40 °C. *J. Chem. Soc., Faraday Trans. 1* **1978**, *74*, 2070–2076.
- Ding, M. S. Liquid-Solid Phase Diagrams of Ternary and Quaternary Organic Carbonates. *J. Electrochem. Soc.*, in press.
- Liu, Z.-K. Thermodynamic Modeling of Organic Carbonates for Lithium Batteries. *J. Electrochem. Soc.* **2003**, *150*, A359–A365.
- Ding, M. S.; Xu, K.; Jow, T. R. Liquid-Solid Phase Diagrams of Binary Carbonates for Lithium Batteries. *J. Electrochem. Soc.* **2000**, *147*, 1688–1694.
- Ding, M. S.; Xu, K.; Zhang, S.-S.; Jow, T. R. Liquid/Solid Phase Diagrams of Binary Carbonates for Lithium Batteries, Part II. *J. Electrochem. Soc.* **2001**, *148*, A299–A304.
- Ding, M. S. Thermodynamic Analysis of Phase Diagrams of Binary Carbonates Based on a Regular Solution Model. *J. Electrochem. Soc.* **2002**, *149*, A1063–1068.
- Ding, M. S.; Xu, K.; Jow, T. R. Phase Diagram of EC-DMC Binary System and Enthalpic Determination of Its Eutectic Composition. *J. Therm. Anal. Calorim.* **2000**, *62*, 177–186.
- Electrolyte Data Collection, Part 1d, Conductivities, Transference Numbers and Limiting Ionic Conductivities of Aprotic, Protophobic Solvents II. Carbonates*; Barthel, J., Neueder, R., Eds.; DECHEMA: Frankfurt, 2000; Chemistry Data Series, Vol. XII.
- Ding, M. S.; Xu, K.; Zhang, S. S.; Amine, K.; Henriksen, G. L.; Jow, T. R. Change of Conductivity with Salt Content, Solvent Composition, and Temperature for Electrolytes of LiPF₆ in Ethylene Carbonate-Ethyl Methyl Carbonate. *J. Electrochem. Soc.* **2001**, *148*, A1196–A1204.
- Ding, M. S.; Jow, T. R. Conductivity and Viscosity of PC-DEC and PC-EC Solutions of LiPF₆. *J. Electrochem. Soc.* **2003**, *150*, A620–A628.
- Barthel, J.; Meier, R.; Conway, B. E. Density, Viscosity, and Specific Conductivity of Trifluoromethanesulfonic Acid Monohydrate from 309.15 K to 408.15 K. *J. Chem. Eng. Data* **1999**, *44*, 155–156.
- Barthel, J.; Buestrich, R.; Carl, E.; Gores, H. J. A New Class of Electrochemically and Thermally Stable Lithium Salts for Lithium Battery Electrolytes. II. Conductivity of Lithium Organoborates in Dimethoxyethane and Propylene Carbonate. *J. Electrochem. Soc.* **1996**, *143*, 3565–3571.
- Barthel, J.; Gores, H. J.; Schmeer, G. The Temperature Dependence of the Properties of Electrolyte Solutions. III. Conductance of Various Salts at High Concentrations in Propylene Carbonate at Temperatures from -45 °C to +25 °C. *Bunsen-Ges. Phys. Chem.* **1979**, *83*, 911–920.
- Chen, H. P.; Fergus, J. W.; Jang, B. Z. The Effect of Ethylene Carbonate and Salt Concentration on the Conductivity of Propylene Carbonate/Lithium Perchlorate Electrolytes. *J. Electrochem. Soc.* **2000**, *147*, 399–406.
- Gu, G. Y.; Bouvier, S.; Wu, C.; Laura, R.; Rzeznik, M.; Abraham, K. M. 2-Methoxyethyl (Methyl) Carbonate-Based Electrolytes for Lithium Batteries. *Electrochim. Acta* **2000**, *45*, 3127–3139.
- Gu, G. Y.; Laura, R.; Abraham, K. M. Conductivity-Temperature Behavior of Organic Electrolytes. *Electrochem. Solid-State Lett.* **1999**, *2*, 486–489.
- Ue, M.; Mori, S. Mobility and Ionic Association of Lithium Salts in a Propylene Carbonate-Ethyl Methyl Carbonate Mixed Solvent. *J. Electrochem. Soc.* **1995**, *142*, 2577–2581.
- Ue, M. Mobility and Ionic Association of Lithium and Quaternary Ammonium Salts in Propylene Carbonate and γ -Butyrolactone. *J. Electrochem. Soc.* **1994**, *141*, 3336–3342.

- (35) Matsuda, Y.; Nakashima, H.; Morita M.; Takasu, Y. Behavior of Some Ions in Mixed Organic Electrolytes of High Energy Density Batteries. *J. Electrochem. Soc.* **1981**, *128*, 2552–2556.
- (36) Casteel, J. F.; Amis, E. S. Specific Conductance of Concentrated Solutions of Magnesium Salts in Water-Ethanol System. *J. Chem. Eng. Data* **1972**, *17*, 55–59.
- (37) Ding, M. S. Conductivity and Viscosity of PC-DEC and PC-EC Solutions of LiBF₄. *J. Electrochem. Soc.* **2004**, *151*, A40–A47.
- (38) Choquette, Y.; Brisard, G.; Parent, M.; Brouillette, D.; Perron, G.; Desnoyers, J. E.; Armand, M.; Gravel, D.; Slougui, N. Sulfamides and Glymes as Aprotic Solvents for Lithium Batteries. *J. Electrochem. Soc.* **1998**, *145*, 3500–3507.

Received for review March 20, 2004. Accepted April 21, 2004.

JE0498863